Characterizing Carbon Fiber Conductivity for Structural Antenna Applications

Ankur Patil, *Student Member, IEEE*, Emily J. Arnold, *Member*, *IEEE*

***Abstract*— This study explores the potential applications of carbon fiber composite material for structural antennas. Carbon fiber composite materials provide excellent specific strength and stiffness, however, their electrical properties such as conductivity are not well established, especially in the very high frequency range. Knowledge of a material's conductivity is required for electrical performance estimation through simulations. Through combined experimental and simulated analysis of multiple carbon fiber antennas, the effective conductivity for a biaxial weave carbon fiber composite was determined to be between 7,000-13,000 S/m in the very high frequency spectrum. Carbon fiber antenna performance is found to be particularly sensitive to the contact between the carbon fibers and the copper feed; however, radiation efficiencies of carbon fiber composite antennas are found to be within 2-10% of a geometrically identical copper antenna, and their bandwidths are nearly identical. The electrical performance of carbon fiber composite antennas demonstrates significant promise for structural antenna applications in the very high frequency range.**

***Index Terms*— Carbon Fiber Composite Materials, Carbon Fiber Antennas, CFRP Conductivity, Unmanned Aerial System**

I. Introduction

ADVANCED Carbon Fiber Reinforced Plastic (CFRP) composite materials consist of high strength carbon filaments embedded in a low strength polymer matrix. Due to advantageous mechanical properties (such as high specific strength and stiffness), applications of CFRP in the aerospace industry have increased significantly. Over the last 70 years, CFRP has gradually replaced metallic primary and secondary structures in aircraft ranging in size from large transport jets to small Unmanned Aerial Systems (UAS). Efforts to leverage the electrical properties, including conductivity, are much more recent. In the late 1990s and early 2000s there was a significant effort to characterize the material's electrical properties for Electromagnetic Interference (EMI) shielding applications [1]-[5]. The electrical properties of CFRP have also been investigated for other applications, such as structural-health monitoring [6]-[7] and antennas (either as radiating elements or as ground planes) [8]-[13].

Carbon fibers are commercially available in various product forms, such as unidirectional tapes, continuous tows, short fibers, braids, woven fabrics, and hybrid cloths. As with mechanical properties, it is difficult to pinpoint the electrical properties of CFRP due to the large number of design variables associated with the material. Table I provides a summary of CFRP conductivity values found in literature. Most CFRP materials investigated are unidirectional (UD) tape. Similar to mechanical properties, the conductivity is highly dependent on fiber orientation [14], [15]. Studies reporting both the longitudinal and transverse conductivity agree that conductivity is much higher in the longitudinal direction [8], [12], [17]-[21]. The wide range of properties reported are due not only to the variability in the product forms, but also to the somewhat inherently random nature of the material and the various measurement techniques. Composite materials are somewhat random, as the electrical path depends on the fibers and contacts between them. If the carbon fibers of UD tape were perfectly straight after curing and the adjacent fibers did not contact each other, the CFRP component would be highly insulating, especially in the transverse direction. However, due to the curing process, fibers tend to become wavy and resin does not necessarily get infused between each individual fiber, thus creating fiber-to-fiber contacts. Woven cloths have improved fiber-to-fiber contact; however, they have a lower fiber volume in the longitudinal direction which has been shown to be directly related to conductivity [16].

For measurement methods that use contact probes, the polymer matrix material that covers the conductive fibers acts as an insulator – making it difficult to ensure good electrical connectivity. For many DC techniques, a small amount of the matrix material is removed to expose the fibers or conductive adhesives are added to the surface. Even in these cases it is

TABLE I
CFRP CONDUCTIVITIES FOUND IN LITERATURE

Product Form	Frequency Range	Longitudinal Conductivity, S/m	Transverse Conductivity, S/m	Ref.
Tape	8-12 GHz	4,000-10,000	1,000-2,000	[8]
Tape	8-12 GHz	30,000-51,000	-	[9]
Braid	-	8,000	-	[12]
Tape	-	5,000	10	[12]
Tape	1.7-10 GHz	600-5,600	-	[15]
Tape	0.01-100 MHz	30,500-42,600	-	[15]
Tape	DC	3,700-5,500	-	[16]
Tape	1 kHz/DC	41,800	4.7	[17]
Tape	DC	21,190-34,130	2-24	[18]
Tape	DC	44,287	50	[19]
Tape	1 kHz/DC	16,280	18.2	[20]
Tape	-	25,000-50,000	7.7-15.2	[21]

Manuscript received XXXX. This work was supported, in-part, by NSF award OPP-1848210

The authors are with the Department of Aerospace Engineering, University of Kansas, Lawrence, KS, 66045, USA. (e-mail: ankurpatil@ku.edu, earnold@ku.edu).

difficult to guarantee excellent connections [30], nor does it accurately reflect the condition in which the material is used (one of the roles of the matrix in a composite is to protect the load-bearing fibers, thus removing it is discouraged). The standard waveguide technique is the most common approach for AC conductivity measurements and does not require electrical contact with a probe; however, this approach is typically limited to Ultra-High Frequencies (UHF) [8], [9] and higher due to the limitations and availability of waveguides that operate at lower frequencies.

From Table I, it is clear that there is lack of research on CFRP conductivity at frequencies between the Ultra High Frequency (UHF) spectrum and DC. This paper addresses the gap in conductivity information and presents a novel experimental method for evaluating the effective conductivity of CFRP in the VHF spectrum to accurately predict the electrical performance of antennas operating in this spectrum. This work is motivated by future applications of structural antennas, particularly with regards to UAS. The primary structures of small- to medium-scale UASs can potentially be used as antennas (such as spars made of CFRP material). This offers twofold weight saving for a UAS by eliminating the antenna's weight and replacing a metallic antenna with a lighter CFRP antenna. Typically, UAS with maximum take-off weights of 80-100 lbs. have payload capacities of around 10-20 lbs., so even a few ounces in weight savings is significant. Multifunctional load-bearing antenna structures will also eliminate additional weight and drag caused by antenna-supporting structures. The VHF spectrum is of particular interest for UAS applications as many remote sensing missions utilize VHF [22]-[24]. In addition, legacy communication and navigation networks used by manned aircraft operate in the VHF spectrum, and thus many exciting new UAS technologies could leverage these networks.

Given the targeted structural antenna application, the method presented also considers the sensitivity of the feeding approach when determining the conductivity. Feeding a CFRP structural antenna proves to be difficult because soldering to the material is not possible. While electrodeposition processes can be used for metalizing the dry carbon [25], this effect is negated when mixed with the matrix polymer. In other instances, carbon nanotubes [26]-[28] or silver nanoparticles [29] have been added to the resin system; however, these approaches significantly increase cost and do not guarantee adequate connection [30]. For our experimental analysis, we have used embedded copper strips that are co-cured with the laminate. It is important to estimate the conductivity of the CFRP in the usable form for antenna applications, and since the conductivity is sensitive to the feeding technique, we describe it as the "effective conductivity."

To the authors' knowledge, this paper represents the first targeted effort to determine CFRP conductivity and thoroughly characterize antenna performance in the VHF range. Section II of this paper includes a conductivity analysis of a CFRP material using an experimental technique at multiple VHF frequencies. In Section III, CFRP antenna performance is discussed in detail and its electrical properties are compared with a metallic (copper) antenna. Another experimental analysis to determine the sensitivity of CFRP conductivity to feeding technique is discussed in Section IV, and the conclusions of the study are summarized in Section V.

II. CFRP Conductivity Experimental Analysis

A. Method Overview

In this sub-section, we discuss a new experimental technique to bound the CFRP conductivity values for the VHF band via the antenna's S_{11} parameter. In the past, efforts have been made to determine conductivity of composite material via the S_{11} parameter in the Ultra to Super High Frequency (SHF) ranges through waveguide techniques [8]. While the S_{11} measurement in [8] was that of a guided wave reflecting off the surface of a CFRP panel, the S_{11} measurement used in this technique is a function of the impedance mismatch of the antenna and the source. The input impedance of an antenna, Z_a is given by (1),

$$Z_a = R_a + jX_a \tag{1}$$

where, R_a and X_a are the antenna resistance and reactance, respectively, in ohms. The antenna resistance can be broken down into the sum of the radiation resistance, R_r, and the loss resistance, R_L. For a dipole with a cross-section much larger than the skin depth ($\delta = \sqrt{2 / (\omega\mu_0\sigma)}$), the current is confined to a thin layer near the surface. The loss resistance can be written as [31],

$$R_L = \frac{l}{P}\sqrt{\frac{2\pi f\mu_0}{2\sigma}} \tag{2}$$

where l is the length of the antenna, P is the perimeter of the cross section, f is the frequency, μ_0 is the free space permeability, and σ is the material conductivity. Given the relationship between the antenna's conductivity and input impedance, the effective conductivity can be determined by varying the conductivity in a finite element analysis and comparing the response to measurements from an equivalent antenna.

A copper (Cu) antenna was used as a reference/baseline to compare the electrical performance of CFRP antennas due to the well-known conductivity ($58\text{x}10^6$ S/m). As shown in Fig. 1, the Cu antenna was fed with a short length of coax line. The Cu antenna was first simulated in the Ansys HFSS software [32] to determine the geometry of an antenna that could resonate at the desired frequency. While dipoles are very simple to model in commercially available simulation software, the geometric abstractions for the feeding mechanism can affect the simulated results. To verify the accuracy of the feed geometry modeled in the simulation, dipole antennas were first built and

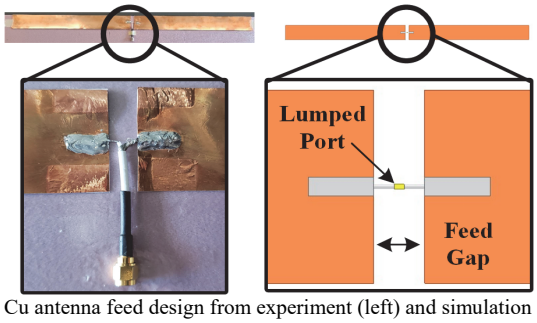

Fig. 1. Cu antenna feed design from experiment (left) and simulation (right).

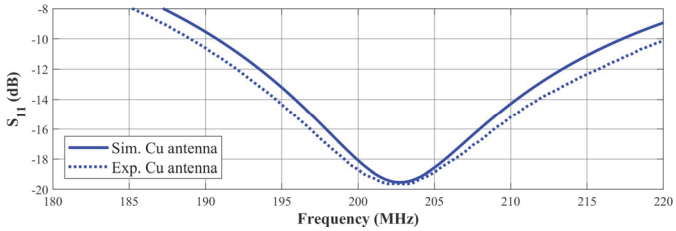

Fig. 2. S_{11} results of Cu antenna

simulated with copper material, as shown in Fig. 1. In the simulation, the feed was modeled as a lumped port with 50 Ω impedance connected to two small cylinders and rectangular blocks. Both the cylinders and blocks were given perfect electric conductor properties and represent the feed cable arms and solder. To capture the effects of feeding the dipole with the coax line on the antenna input impedance, the feed gap shown in Fig. 1 was varied in the Cu antenna model until the S_{11} from the simulation results matched the experimental results. This was repeated for each antenna analyzed. Fig. 2 shows the tuned S_{11} from the simulation and experimental results for a copper antenna resonating at 202 MHz. An identical feed geometry was then used in the associated CFRP model so the effect of the feeding technique on antenna performance could be properly accounted for in the simulations. While it is recognized that the use of a balun is a more common approach to feeding a dipole, the inclusion of a balun will affect the resultant S_{11} due to the component's insertion loss, input return loss, and coupling between the balun and antenna. For this reason, it was determined it would be easier to capture the effects of the feeding technique using the approach described above. The close match in S_{11} between the simulated and experimental results indicate there is good impedance predictions by the simulation at resonance.

With a baseline Cu antenna design, a geometrically equivalent CFRP antenna was fabricated to see how well it could resonate at VHF frequencies. As mentioned above, one challenge with a CFRP antenna design is the difficulty in feeding the antenna since soldering to CFRP without special treatments is not practical. An embedded copper strip, shown in Fig. 3, was used to feed the antenna, where a feeding coax cable was soldered onto the exposed Cu strip on the dipole arms. The CFRP antenna was fabricated from an AS4 bi-axial plain weave (0°/90°) fabric with a wet layup technique (DPL 40 epoxy resin) and cured at room temperature. The S_{11} and gain properties of the fabricated CFRP antenna were measured in an anechoic chamber using a Vector Network Analyzer (VNA). The CFRP antenna was then simulated in HFSS with CFRP conductivity varying from 2,000-20,000 S/m through a parametric analysis. The effective CFRP conductivity was found by matching the simulated S_{11} at resonance with the experimental S_{11}. The effective CFRP conductivity range corresponding to a S_{11} variation of ±0.5 dB was also found to account for the

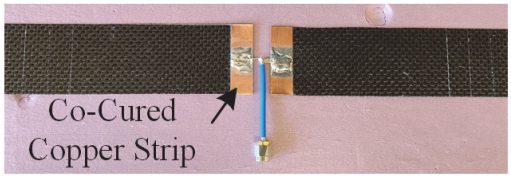

Fig. 3. Close up view of CFRP SL antenna

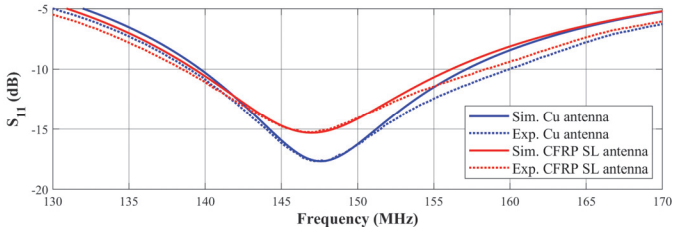

Fig. 4. HFSS vs. Experimental S_{11} plots for Cu and CFRP SL antenna at 148 MHz (@ σ_{CFRP}= 10,800 S/m)

variability in antenna design, such as fiber-fiber contact and fabrication technique.

B. Results for CFRP Effective Conductivity

The effective CFRP conductivity analysis was performed at multiple frequencies in the VHF frequency range of 150-250 MHz to study the sensitivity of the conductivity to frequency. A single-layer CFRP antenna design with 12.7 mm (0.5 in.) embedded Cu strip at the feed location (referred as 'CFRP SL Antenna') was fabricated for this analysis considering its design simplicity and easy manufacturing aspects. To reduce variability in the antenna design and avoid fabrication of multiple antennas operating at multiple frequencies, an initial CFRP SL antenna was designed to operate at 150 MHz. The dimensions of this antenna were 909.3 mm x 40.6 mm (35.8 in. x 1.6 in.). Fig. 4 shows the matched simulated and experimental S_{11} plots for the CFRP and Cu antennas resonating at 148 MHz. The antenna length was then subsequently trimmed to match frequencies up to 250 MHz, while maintaining a constant antenna width. At each chosen frequency, the conductivity analysis procedure was repeated.

Using the S_{11} as the matching metric, we compared the experimental results to the simulated results to determine the effective conductivity range for the CFRP SL antenna at various frequencies. Table II summarizes the effective CFRP conductivity that best matched the experimental results. The table also includes the conductivity range corresponding to a S_{11} variation of ±0.5 dB at their respective resonating frequencies. The approximate effective conductivity for CFRP material was determined to be between 7,000-13,000 S/m for the frequency range of 150-250 MHz. For a S_{11} variation of ±0.5 dB, the corresponding effective conductivity ranged from 5,700-18,500 S/m in this frequency range, as shown in Table II. Fig. 5 shows the trendline for the effective CFRP conductivity along with range bars corresponding to the ±0.5 dB S_{11} variation. The negative slope of the trendline would indicate that the effective conductivity slightly decreases with

TABLE II
EFFECTIVE CONDUCTIVITY OF CFRP ANTENNAS

Resonating Frequency, MHz	Experimental S_{11} at Resonance, dB	Approximated Effective Conductivity, S/m	Effective Conductivity Range for S_{11} Variation of ±0.5 dB, S/m
148	-15.27	11,000	8,300 - 14,500
158	-16.35	13,000	8,200 - 18,500
173	-16.90	8,000	6,600 - 10,100
187	-16.95	8,500	6,800 - 11,000
204	-17.69	7,000	5,700 - 8,600
221	-18.89	10,000	7,600 - 13,000
243	-19.00	7,000	5,700 - 8,500

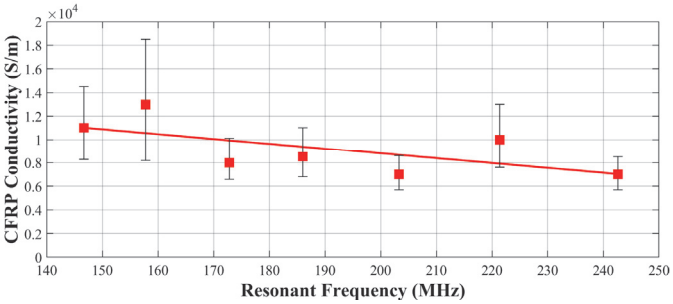

Fig. 5. CFRP effective conductivity and range from Table II

increasing frequency for CFRP materials. This decreasing trend in conductivity agrees with what has been found in other investigations of frequencies above 1.7 GHz [8], [15]; this phenomenon has been attributed to increases in reactance due to magnetic flux changes from neighboring fibers.

When using the respective conductivity values reported in Table II for a VHF antenna simulation, it is expected that the S_{11} and resonating frequency would be within 1 dB and 1.1 MHz (given the variability in effective conductivity over the frequency range). As the resonating frequency increased from 148 MHz to 243 MHz, the variation in the S_{11} and effective conductivity were found to be 3.7 dB and 6,100 S/m, respectively.

C. Validation of Approach Using the Wheeler Cap Method

To validate the results presented in the previous sections, the conductivity for CFRP was determined using a Wheeler Cap method similar to the approach described in [9]. Given the Wheeler Cap method is better suited for antennas with ground planes, after the final trimming of the CFRP antenna from II.B, the dipole was deconstructed and converted to a monopole. As shown in Fig. 6a, the planar CFRP monopole with dimensions 264 mm x 40.6 mm (10.4 in. x 1.6 in) was fed with the same coax line and installed on a square ground plane with side lengths of 845 mm. A copper equivalent monopole was also constructed to serve as a reference to determine system losses. To determine the loss resistance, radiation efficiency, and conductivity of a finite conductivity material using the approach in [9], the S_{11} of the monopole is first measured in free space. The measurement is then repeated with the Wheeler cap installed over the antenna, and the resulting antenna resistance is assumed to be the loss resistance, R_L (i.e. the radiation resistance, R_r, is assumed to be zero). The radiation efficiency, RE, is found using the input resistance, R_{in}, (free space measurements) and the loss resistance at the free space resonance using (3)

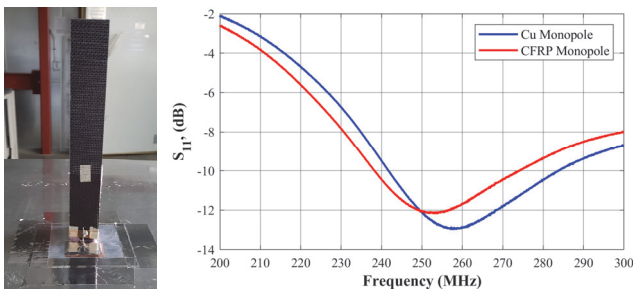

(a) (b)

Fig. 6. CFRP planar monopole installed on ground plane (a), and measured S_{11} for both Cu and CFRP monopoles (b).

$$RE = \frac{R_{in}-R_L}{R_{in}} \quad (3)$$

where $R_{in}=R_r+R_L$. The conductivity is subsequently found using the loss resistance and Eq. (12) from [9].

Fig. 6b shows the measured free space S_{11} for both the CFRP and Cu monopole antennas. As was done in [9], to determine the losses caused by the Wheeler cap and experimental setup, the Cu monopole antenna was first simulated in HFSS both with and without the Wheeler cap. The Wheeler cap used for the measurements was a box constructed from 0.4 mm thick aluminum with dimensions 660 mm x 400 mm x 400 mm. Table III summarizes the simulated and experimental results for the Cu monopole. The resonance frequencies matched within ~1 MHz; however, the loss resistances determined from the Wheeler cap measurement/simulations differed by 1.91 Ω. As discussed in [9], this difference is attributed to the losses from the Wheeler cap, and should be used to correct the measured loss resistance of the CFRP antenna.

To determine the current distribution on the planar monopole (necessary for calculating the material conductivity using Eq. (12) from [9]), an HFSS model of the CFRP monopole was also constructed. This model was not only used to determine the current distribution, but also served as a means to check the conductivity value determined from the measurements. Table III also summarizes the simulated and experimental results for the CFRP monopole. Note that the loss resistance reported for the measurement is the corrected loss resistance (i.e. actual measured resistance was 7.7 Ω). Using the corrected CFRP loss resistance, the conductivity was found to be 7,200 S/m. As shown in Table III, when this conductivity was used in the HFSS simulation, there was very good agreement in resonance frequency, radiation efficiency, and loss resistance. In addition, the conductivity found for the CFRP using the Wheeler cap method is well within the ranges reported in II.B, and the reduction in radiation efficiency is expected, thus giving confidence for the proposed methodology and reported conductivity.

III. CFRP VHF Antenna Performance

With a range of conductivity values established, the performance of the CFRP antennas were more closely examined to determine the efficacy of future structural antenna applications. The planar copper antenna was once again used as a baseline for comparison with the CFRP planar antennas.

Fig. 7 shows the S_{11} at resonance over the frequency range for the Cu antenna and the CFRP SL antenna. Both of these antennas had a decreasing trend with increasing resonating frequency. These trendlines connecting the S_{11} at the

TABLE III
EFFICIENCY, R_L, AND CONDUCTIVITY USING WHEELER CAP METHOD

Method	Frequency (MHz)	Efficiency (%)	R_L (Ω)	Conductivity (S/m)
		Copper		
Simulation	256.2	99.9	0.047	$58x10^6$
Measurement	257.3	96.7	1.96	$58x10^6$
		CFRP		
Simulation	253.0	88.6	5.90	7,200
Measurement	253.2	89.9	5.85	7,200

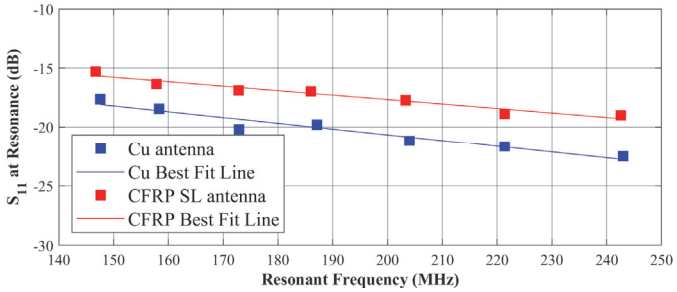

Fig. 7. Experimental S_{11} values at the antenna resonances

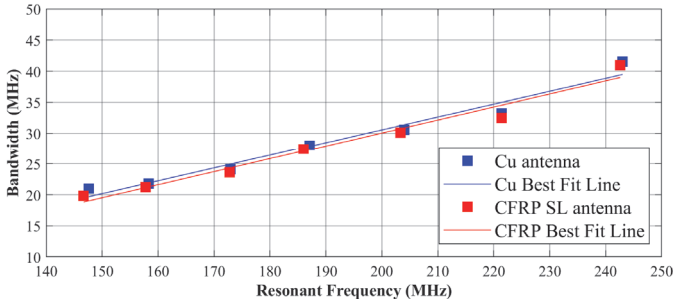

Fig. 8. Experimental antenna 10-dB bandwidths over the frequency range

resonances for the Cu antennas and the CFRP antennas were nearly parallel with a nearly constant offset ~3 dB, which can be attributed to lower CFRP conductivity (and thus higher losses and worse match). The slight variation in the slopes is again likely due to the decreasing trend of CFRP conductivity over the frequency range. For both antenna designs, the decreasing length to width (L/W) ratio with an increasing resonating frequency offered improved impedance matching, and in general is not attributed to the material's conductivity.

Fig. 8 shows that the 10-dB impedance bandwidths of both antennas were essentially identical and increased with increasing resonating frequency. It is clear from this plot that the 10-dB bandwidth of the CFRP antenna was not affected by the lower conductivity of the CFRP material. While the length of the antennas was trimmed to achieve a higher resonance, the width was not modified. Thus, the antenna bandwidths for both antennas improved with increasing resonant frequency due to the decreasing L/W ratio of the antennas.

The CFRP SL antenna gain was measured in an anechoic chamber by using the Cu antenna as the reference antenna and assuming a gain of 2.2 dBi. The gains of the CFRP antennas were determined to be between 1.75-2 dBi for the frequency range, which is 0.2-0.45 dB lower (radiation efficiency 5-10% lower) than the Cu antenna, as shown in Table IV. For a radiation efficiency of 96% for the Cu antenna, the radiation efficiencies for the CFRP antennas were derived and plotted in Fig. 9. The table and plot show a relatively constant radiation efficiency, which suggests a relatively small change in effective conductivity over the frequency range of 150-250 MHz. This also suggests that a CFRP antenna can radiate at VHF frequencies with only a marginal loss as compared to a Cu antenna. The experimental and simulated gain values of the CFRP SL antenna also matched very well over the frequency range with a negligible gain variation of 0.12 dBi. The sensitivity of the simulated gain value to the effective CFRP conductivity range (referring to Table II) was 0.23 dBi over the frequency range.

TABLE IV
CFRP ANTENNA GAINS AND Δ% EFFICIENCY AT VHF FREQUENCIES

Resonant Frequency, (MHz)	Gain, (dBi)	Δ% Efficiency Decrease Compared to Cu Antenna
148	1.78	9.2
158	1.96	5.4
173	1.83	8.2
187	1.92	6.2
204	1.86	7.5
221	1.85	7.7
243	1.88	7.1

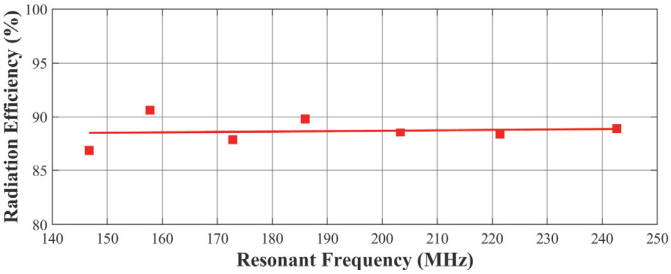

Fig. 9. Experimental RE values at the antenna resonances

Given the range of effective conductivity variation, the antennas made of CFRP material showed excellent electrical performance in terms of antenna gain, bandwidth, and radiation efficiency. Matching of experimented and simulated electrical properties further ensures the potential of CFRP cloth materials for VHF antenna applications. A CFRP conductivity range of 5,700-18,500 S/m (determined in this study) can be used in EM simulations, and the resulting antenna S_{11} can be expected to be within ±0.5 dB.

IV. SENSITIVITY OF EFFECTIVE CONDUCTIVITY TO ANTENNA FEEDING TECHNIQUE

In this sub-section, we discuss the sensitivity of the antenna measurement to the copper feed design. To investigate this sensitivity, a length of copper strip embedded between two CFRP layers was varied from 12.7 mm (0.5 in.) to 38.1 mm (1.5 in.), as described in Table V. Multiple CFRP antennas were fabricated with the same fabric and curing technique discussed earlier. In design 'A', a piece of 12.7 mm (0.5 in.) Cu tape was adhered to the CFRP surface post-cure. For the rest of the CFRP designs, copper strips were co-cured/embedded onto CFRP surfaces, while a 12.7 mm (0.5 in.) section of the Cu strip was left exposed for soldering.

The CFRP antennas were designed to operate around 200 MHz, and the corresponding dimensions were 655.3 mm x 40.6 mm (25.8 in. x 1.6 in.). The S_{11} of the CFRP antenna designs

TABLE V
CFRP ANTENNA DESIGNS

Design	Antenna Description
A	Single-layer CFRP cloth with 12.7 mm (0.5 in.) adhesive copper tape contact
B	Single-layer CFRP cloth with 12.7 mm (0.5 in.) embedded copper strip contact
C	Double-layer CFRP cloth with 12.7 mm (0.5 in.) embedded copper strip contact
D	Double-layer CFRP cloth with 25.4 mm (1 in.) embedded copper strip contact
E	Double-layer CFRP cloth with 38.1 mm (1.5 in.) embedded copper strip contact

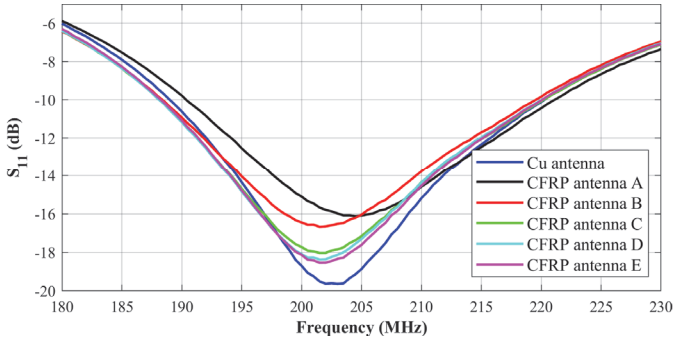

Fig. 10. CFRP antenna S_{11} plots from experiment

were measured and plotted in Fig. 10, and the gain performance is summarized in Table VII.

While the Cu antenna and all five CFRP antennas resonated around 202 MHz with about 27 MHz bandwidth, the sensitivity to the feeding technique was apparent. As expected, the Cu antenna delivered the lowest S_{11} value of -19.61 dB, due to better impedance matching at resonant frequency and good connectivity between the coax cable and antenna arms. The CFRP antenna design 'A' had the worst match with a S_{11} value of -16.12 dB at resonance. This was expected due to the less effective 'fiber-metal' contact between the CFRP material and the Cu tape feed since the tape was simply adhered to the CFRP surface post-cure. For the design 'B', co-curing the Cu strip on top of the CFRP layer resulted in 0.5 dB improvement in S_{11} over design 'A'.

The CFRP antenna designs 'C', 'D', and 'E', which each had double CFRP layers, provided further improvement of 1.4-1.9 dB in S_{11} due to increased fiber-metal contact as compared to previous designs. The double-layer CFRP antennas showed a slight increase in 10-dB bandwidth with increasing fiber-metal contact as the copper feed size increased from 12.7 mm (0.5 in.) to 38.1 mm (1.5 in.). However, the improvements in bandwidths were not significant, and CFRP antennas delivered similar bandwidths as the Cu antenna.

Following the S_{11} measurements, pattern and gain measurements were taken in an anechoic chamber to study the sensitivity of the CFRP feed design. All the antennas exhibited the toroid/doughnut shaped radiation pattern typical of a dipole, and the gain values for all CFRP antenna designs were calculated at their resonant frequency using the Cu antenna as a reference antenna with an assumed gain of 2.2 dBi. Table VII summarizes the measured gain and relative efficiency values.

The radiation efficiencies of all CFRP antenna designs were again found to be within 10% of the Cu antenna, and they had a similar improving gain trend with fiber-metal contact as the S_{11}. Both of these attributes imply that the antenna performance is sensitive to the feeding design or quality of the fiber-metal contact. For the double-layered CFRP antenna designs, the connectivity was improved because the fibers were touching both sides of the feed.

The CFRP antennas were simulated with the same feeding design from Section II, and the simulated and experimental S_{11} results were compared to determine the effective conductivity for all the CFRP antenna designs. We performed a parametric analysis for each CFRP antenna design, where the conductivity value of the CFRP dipole arms were varied from 2,000-15,000 S/m, as shown in Fig. 11 (dashed line represents experimental data). The simulated radiation efficiencies of the CFRP

TABLE VII
CFRP ANTENNA GAINS AND Δ% EFFICIENCY COMPARISON

Antenna Design	Gain, (dB)	Δ% Efficiency Decrease as Compared to Cu Antenna
CFRP antenna 'A'	1.76	9.6
CFRP antenna 'B'	1.81	8.6
CFRP antenna 'C'	1.96	5.4
CFRP antenna 'D'	2.09	2.5
CFRP antenna 'E'	2.14	1.4

antennas were also within 10% of the simulated Cu antenna, which agreed well with the experimental analysis (Table VII).

The approximated effective conductivity was determined for each CFRP antenna design along with the conductivity range corresponding to a S_{11} variation of ±0.5 dB, as shown in Table VII. As expected, the CFRP antenna 'A' delivered the lowest CFRP conductivity range due to the poor fiber-metal contact, while the rest of the CFRP antennas exhibited an effective conductivity in the range of 8,000-10,000 S/m. The effective conductivities of the CFRP antennas were directly related to the extent of the fiber-metal contact.

A S_{11} variation of ±0.5 dB was observed for an effective conductivity range of 4,800-20,000 S/m at 200 MHz across the various feeding designs. The conductivity values in Table VI are within the same range as the values found in Table II. When using these conductivity values for a VHF rectangular planar antenna simulation, the S_{11} and resonating frequency could be predicted within 1 dB and 0.5 MHz.

V. CONCLUSION

The effective conductivity values for CFRP material is within the same range as other woven or braided fabric conductivity values found in literature. In particular, the values match very well with the bi-axial material reported in Table I (8,000 S/m). It is clear that the effective conductivity is very sensitive to the feeding technique of the antenna; thus, it is important that the effective conductivity values are used in simulations to include the effects of the fiber-metal contact. Given the intended

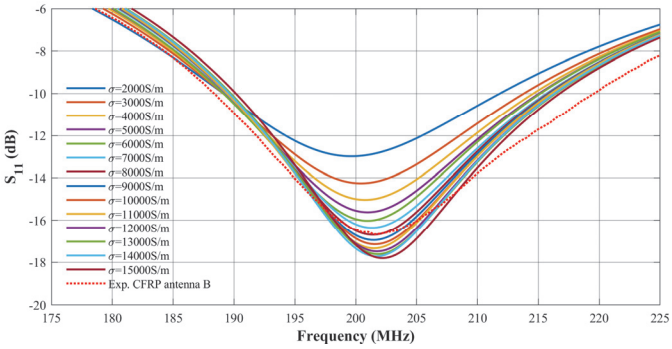

Fig. 11. S_{11} plots for CFRP antenna design 'B' from parametric analysis

TABLE VI
EFFECTIVE CONDUCTIVITY OF CFRP ANTENNA DESIGNS

Antenna Design	Approximated Effective Conductivity, S/m	Effective Conductivity Range for S_{11} variation of ±0.5 dB, S/m
Cu Antenna	58×10^6 (Theoretical)	58×10^6 (Theoretical)
CFRP antenna 'A'	6,000	4,800 - 7,300
CFRP antenna 'B'	8,000	6,500 - 10,000
CFRP antenna 'C'	8,300	5,700 - 13,000
CFRP antenna 'D'	9,000	6,000 - 17,000
CFRP antenna 'E'	10,000	6,000 - 20,000

application of the CFRP conductivities, the effective conductivity values are of much more interest than the true conductivity of the CFRP material. Considering the effects of frequency and fiber-metal contact, the effective conductivity varied between 7,000-13,000 S/m for the planar antennas. To validate the conductivity values found using the dipoles, a Wheeler cap method was used, and the conductivity of a planar CFRP monopole antenna that resonates at 252 MHz was found to be 7,200 MHz, which is well within the identified range. For an effective conductivity range of 5,700-20,000 S/m, the S_{11} of the antenna could be predicted within ±0.5 dB and the resonant frequencies were predicted within 0.5%.

Overall, the performance of the CFRP antennas is very encouraging for future applications of structural antennas. The radiation efficiencies of CFRP antennas were found to be within 10% lower and the bandwidths within 1.5 MHz of that of an equivalent Cu antenna in the VHF frequency range. The electrical performance of the CFRP antenna (namely effective conductivity, S_{11}, and gain values) improved with an increase in the fiber-metal contact. The effective CFRP conductivity and gain values were improved by 4,000 S/m and 0.4 dB, respectively, by increasing the fiber-metal contact at 200 MHz. The S_{11} and radiation efficiency results demonstrate significant promise for using CFRP material for structural antennas in the VHF frequency range.

ACKNOWLEDGMENT

This work was supported, in-part, by NSF award OPP-1848210. We would like to thank Dr. Richard Hale, Mr. Jim Rood, and Mr. Brad Schroeder for their support in helping us fabricate the antennas. We would also like to thank Ms. Rachel James for editing and formatting the manuscript.

REFERENCES

[1] J. R. Gaier, “Intercalated graphite Fiber Composites as EMI Shields in Aerospace Structures," *IEEE Trans. on Electro. Comp.*, vol. 34, no. 3, pp. 351-356, Aug. 1992.

[2] S. Geetha, K. K. Satheesh Kumar, C. R. Rao, M. Vijayan, and D. C. Trivedi, "EMI shielding: Methods and materials—A review," *Journal of Applied Polymer Science*, vol. 112, no. 4, pp. 2073-2086, 2009.

[3] C. L. Gardner and Y. F. C. Poissant, “Measurement of the shielding properties of composite materials: comparison of the dual TEM and noncontact probe methods," *IEEE Trans. on Electro. Comp.,* vol. 40, no. 4, pp. 364-369, Nov. 1998.

[4] M. D’Amore and M. S. Sarto, “Theoretical and experimental characterization of the EMP-interaction with composite-metallic enclosures,” *IEEE Trans. Electro. Comp.*, vol. 42, no. 1, pp. 152–163, Feb. 2000.

[5] S. Sankaran, S. Dasgupta, K. Ravi Sekhar, and M. J. Kumar, "Thermosetting polymer composites for EMI shielding applications," *9th Int’l Conf. on Electro. Interference and Comp. (INCEMIC 2006)*, Bangalore, India, pp. 1-6, 2006.

[6] S. Wang, D. Wang, D. D. L. Chung, and J. H. Chung, “Method of sensing impact damage in carbon fiber polymer-matrix composite by electrical resistance measurement,” *Journal of Mat’l Sci.*, vol. 41, pp. 2281–2289, 2006.

[7] X. E. Gros and K. Takahashi, "Monitoring delamination growth in CFRP materials using eddy currents," *Nondestructive Testing and Evaluation,* vol. 15, no. 2, pp. 65-82, 1998.

[8] A. Galehdar, W. S. Rowe, K. Ghorabni, P. J. Callus, S. John, and C. H. Wang, “The effect of ply orientation on the performance of antennas in or on carbon fiber composites," *Progress in Electromagnetics Research*, vol. 116, pp. 123-136, Apr. 2011.

[9] A. Galehdar, P. J. Callus, and K. Ghorbani, “A Novel Method of Conductivity Measurements for Carbon Fiber Monopole Antenna," *IEEE Trans. on Antennas and Propag.*, vol. 59, no. 6, pp. 2120-2126, Jun. 2011.

[10] S. S. Yoon, J. W. Lee, T. K. Lee, J. H. Roh, H. I. Kim, and D. W. Yi, “Conductivity evaluation of a newly proposed material for a SAR reflector antenna,” *Journal Electro. Engineering and Sci.*, vol. 14, no. 3, pp. 293–298, Sep. 2014.

[11] S. S. Yoon, J. W. Lee, T. K. Lee, and J. H. Roh, “Insensitivity Characteristics in the Dual Polarization of Deployable CFRP Reflector Antennas for SAR,” *IEEE Trans. on Antennas and Propag.*, vol. 66, no. 1, pp. 88-95, Jan. 2018.

[12] A. Mehdipour, C. W. Trueman, A. R. Sebak, and S. V. Hoa, "Carbon-fiber composite T-match folded bow-tie antenna for RFID applications," *IEEE Antennas and Propag. Society Int’l Symp.*, pp. 1-4, 2009.

[13] Y. Bayram, Y. Zhou, J. L. Volakis, B. S. Shim, and N. A. Kotov, "Conductive textiles and polymer-ceramic composites for novel load bearing antennas," *IEEE Antennas and Propag. Society Int’l Symp.*, pp. 1-4, 2008.

[14] T. J. Seidel, A. Galehdar, W. S. T. Rowe, S. John, P.J. Callus, and K. Ghorbani, "The anisotropic conductivity of unidirectional carbon fiber reinforced polymer laminates and its effect on microstrip antennas," *Asia-Pacific Microwave Conference*, pp. 1470-1473, 2010.

[15] H. C. Kim and S. K. See, "Electrical properties of unidirectional carbon-epoxy composites in wide frequency band," *Journal of Physics D: Applied Physics,* vol. 23, no. 7, pp. 916, 1990.

[16] A. Todoroki, M. Tanaka, and Y. Shimamura, "Measurement of orthotropic electric conductance of CFRP laminates and analysis of the effect on delamination monitoring with an electric resistance change method." *Composites Science and Technology*, vol. 62, no. 5, pp. 619-628, 2002.

[17] Y. Hirano, T. Yamane, and A. Todoroki. "Through-thickness electric conductivity of toughened carbon-fibre-reinforced polymer laminates with resin-rich layers," *Composites Sci. and Tech. 122*, pp. 67-72, 2016.

[18] J. C. Abry, S. Bochard, A. Chateauminois, M. Salvia, and G. Giraud. "In situ detection of damage in CFRP laminates by electrical resistance measurements," *Composites Sci. and Tech. 59*, no. 6, pp. 925-935, 1999.

[19] N. Athanasopoulos and V. Kostopoulos. "A comprehensive study on the equivalent electrical conductivity tensor validity for thin multidirectional carbon fibre reinforced plastics," *Composites Part B: Engineering 67*, pp. 244-255, 2014.

[20] Y. Akcin, S. Karakaya, and O. Soykasap, "Electrical, thermal and mechanical properties of CNT treated prepreg CFRP composites," *Mat’l Sci. Application,* vol. 7, pp. 465-83, 2016.

[21] S. Yasufuku and T. Inohara, "Carbon-fiber technology and its application to the electrical industry in Japan," *IEEE Electrical Insulation Magazine 3*, no. 6, pp. 9-18, 1987.

[22] E. Arnold, C. Leuschen, F. Rodriguez-Morales, J. Li, J. Paden, R. Hale, and S. Keshmiri, "CReSIS airborne radars and platforms for ice and snow sounding," *Annals of Glaciology*, no. 81, pp. 1-10, 2019.

[23] A. Mahmood, "Design, Integration, and Deployment of UAS borne HF/VHF Depth Sounding Radar and Antenna System," PhD dissertation, University of Kansas, USA, 2017. [Online]. Available: https://kuscholarworks.ku.edu/handle/1808/25923
J. Q. Shang, J. W. Scholte, and R. K. Rowe, “Multiple Linear Regression of Complex Permittivity of a Till at Frequency Range from 200 MHz to 400 MHz,” *Subsurface Sensing Technologies and Applications*, no. 1, pp. 337–356, 2000.

[24] J. Q. Shang, J. W. Scholte, and R. K. Rowe, “Multiple Linear Regression of Complex Permittivity of a Till at Frequency Range from 200 MHz to 400 MHz,” *Subsurface Sensing Technologies and Applications*, no. 1, pp. 337–356, 2000. Available: https://doi.org/10.1023/A:1010199809583.

[25] M. Nier, T. Böttger, F. Böttger-Hiller, D. Nickel, I. Scharf, D. Nestler, B. Wielage, and T. Lampke, "Metalized carbon fibers for solderable and wear-resistant composite materials," *19th Int’l Conf. on Composite Mat’ls (ICCM)*, Montreal, Canada, 2013.

[26] A. Mehdipour, A. R. Sebak, C. W. Trueman, I. D. Rosca, and S.V. Hoa, "Reinforced continuous carbon-fiber composites using multi-wall carbon nanotubes for wideband antenna applications," *IEEE Trans. on Antennas and Propag.*, vol. 58, no. 7, pp. 2451-2456, July 2010.

[27] A. Mehdipour, I. D. Rosca, A. R. Sebak, C. W. Trueman, and S. V. Hoa, "Carbon nanotube composites for wideband millimeter-wave antenna applications," *IEEE Trans. on Antennas and Propag.*, vol. 59, no. 10, pp. 3572-3578, Oct. 2011.

[28] Y. Lin, M. Gigliotti, M. C. Lafarie-Frenot, and J. Bai, "Effect of carbon nanotubes on the thermoelectric properties of CFRP laminate for aircraft applications," *Journal of Reinforced Plastics and Composites*, vol. 34, no. 2, pp. 173-184, 2015.
[29] E. Kandare, et al., "Improving the through-thickness thermal and electrical conductivity of carbon fibre/epoxy laminates by exploiting synergy between graphene and silver nano-inclusions," *Composites Part A: Applied Science and Manufacturing*, vol. 69, pp. 72-82, 2015.
[30] E. J. Riley, E. H. Lenzing, and R. M. Narayanan, "Characterization of carbon fiber composite materials for RF applications," *Proc. SPIE 9077, Radar Sensor Technology XVIII*, vol. 9077, May 2014. Available: https://doi.org/10.1117/12.2050132.
[31] C. A. Balanis, Antenna theory: analysis and design, 3rd ed. New Jersey, USA: John wiley & sons, pp. 86, 2016.
[32] HFSS, High Frequency Structure Simulator, Software Package, Ansys, Ver. 2016.1, Canonsburg, PA, 2014. Available: https://www.ansys.com/Products/Electronics/ANSYS-HFSS

Ankur S. Patil (M'20) received the B.S. degree in Aeronautical Engineering from the Aeronautical Society of India, Bangalore, India, in 2012 and the M.S. degree in Aerospace Engineering from University of Kansas, KS, USA in 2017. He received his Doctoral Candidacy in Aerospace Engineering at KU in Feb. 2020. He works as a Graduate Research Assistant with the Center for Remote Sensing of Ice Sheets (CReSIS) at KU since 2015. His research interests include the design and manufacturing of antennas for airborne remote sensing in polar regions. His current work is based on designing and integrating multifunctional structural antennas onto unmanned aerial systems (UASs). He placed in the top 10 globally with his team at the 2018 Boeing-sponsored GoFly competition and won first place with his team at the 2015 PESA competition. He is a member of the AIAA and the Aerospace Engineering Honor Society - Sigma Gamma Tau.

Emily J. Arnold (S'12-M'15) received a BS in Aerospace Engineering from the University of Kansas in Lawrence, KS, in 2009, and a PhD from the University of Kansas in 2013. Dr. Arnold is an assistant professor in the Aerospace Engineering Department at KU. She served as the Lead Design and Structural Engineer for several airborne antenna arrays used for remote sensing ice sheets in Antarctica and Greenland. She has extensive experience in building and designing composite structures, including the structure for a 1,100-lb. UAS. In 2019, Dr. Arnold was a CAREER Award recipient. Dr. Arnold was also the recipient of two NASA Earth and Space Science Fellowships, as well as Zonta International's Amelia Earhart Fellowship. Prior to returning to KU as an assistant professor, she worked at the MITRE Corporation.